Bioinformatics and Biology Insights

ORIGINAL RESEARCH

The Role of Electrostatic Interactions on Klentaq1 Insight for Domain Separation

Santi Nurbaiti[1], Muhamad A. Martoprawiro[2], Akhmaloka[1] and Rukman Hertadi[1]

[1]Biochemistry Research Group, Faculty of Mathematics and Natural Sciences, Institut Teknologi Bandung, Indonesia. [2]Inorganic and Physical Chemistry Research Group, Faculty of Mathematics and Natural Sciences, Institut Teknologi Bandung, Indonesia. Corresponding authors email: rukman@chem.itb.ac.id; aan@chem.itb.ac.id

Abstract: We investigated the relationship between the thermostability of Klentaq1 and factors stabilizing interdomain interactions. When thermal adaptation of Klentaq1 was analyzed at the atomic level, the protein was stable at 300 and 350 K. It gradually unfolded at 373 K and almost spontaneously unfolded at 400 K. Domain separation was induced by disrupting electrostatic interactions in two salt bridges formed by Lys354-Glu445 and Asp371-Arg435 on the interface domain. The role of these interactions in protein stability was evaluated by comparing free energy solvation ($\Delta\Delta G_{solv}$) between wild type and mutants. Substitution of Asp371 by Glu or Asn, and also Glu445 by Asn resulted in a positive value of $\Delta\Delta G_{solv}$, suggesting that mutations destabilized the protein structure. Nevertheless, substitution of Glu445 by Asp gave a negative value to $\Delta\Delta G_{solv}$ reflecting increasing protein stability. Our results demonstrate that interactions at the interface domains of Klentaq1 are essential factors correlated with the Klentaq1 thermostability.

Keywords: Klentaq1, domain separation, electrostatic interaction, *in silico* mutation

Bioinformatics and Biology Insights 2012:6 225–234

doi: 10.4137/BBI.S9390

This article is available from http://www.la-press.com.

Introduction

Based on amino acid sequence comparisons and crystal structure analyses, deoxyribonucleic acid (DNA) polymerase (Pol) can be divided into seven groups including A, B, C, D, X, Y, and reverse transcriptase (RT).[1–3] The best studied of these groups is DNA Pol A (or Pol I), including the DNA Pol I of *Escherichia coli (E.coli)*, *Bacillus* DNA Pol I and *Thermus aquaticus* (*Taq*) DNA Pol. These enzymes and their derivatives have been used extensively in biotechnological research, such as for polymerase chain reaction (PCR) research and DNA sequencing.[4]

Taq Pol is an important enzyme that plays a role in DNA repair and recombination *in vivo*.[5] This enzyme was first isolated and characterized by Chien and colleagues.[6] The gene sequence of *Taq* Pol is 38% identical to *E.coli* DNA Pol I,[7] and the gene was cloned and overexpressed in *E.coli* by Kaledin and colleagues as well as Lawyer and colleagues.[8,9] The heterologous enzyme still shows functional activity and its active form is a single monomeric enzyme with a molecular mass of about 93.9 kDa.[9] Biochemical and three-dimensional (3D) structure analysis showed that *Taq* Pol consists of three domains. These domains include 5′→3′ exonuclease (residue number 1–290), 3′→5′ exonuclease (residue number 291–419) and 5′→3′ polymerase (residue number 420–832).[10–12] A 3D structure comparison between *Taq* Pol I and *E.coli* Pol I showed that the C-terminal polymerase domain in both proteins is almost identical, consisting of palm, fingers and thumb subdomains.[13,14] *Taq* Pol I could be digested by a proteolytic enzyme, resulting in a large C-terminal fragment (3′→5′ exonuclease and 5′→3′ polymerase domains) and N-terminal fragment (5′→3′ exonuclease region). The C-terminal fragment is known as the Stoffel Fragment or Klenow *Taq* Pol I (Klentaq1).[4,14] It has been shown that *Taq* Pol I and Klentaq1 have higher thermostability compared to *E.coli* DNA Pol I. As a result, *Taq* Pol I is widely used for amplification of DNA in vitro using PCR. However, this enzyme has lower fidelity compared to *E.coli* DNA Pol I due to lack of a proofreading function motif.[4]

Extensive research on protein thermostability has led to the development of a theoretical foundation and practical applications, especially in the field of protein engineering. Design of mutants with higher thermostability that retain catalytic activity is widely practiced in industry; eg, food, animal feeding, medicine and toiletries.[15] Constructing such mutants is a challenging task because we need to know precisely which key residues/interactions in a protein are responsible for its thermostability and activity.[16] This task can be achieved if we explore the effect of thermal perturbation at the atomic level, which is currently not directly accessible, even after the recent advancement of available instruments. Molecular dynamics (MD) simulation is an alternative approach that provides atomic level information about the effect of thermal perturbation on protein conformation.[17] Key interactions responsible for the maintenance of protein conformation against thermal perturbation can be revealed through examination of the MD simulation trajectory, since we are able to observe gradual thermal unfolding of a protein at the atomic level.

In previous work, we have studied the unfolding process of thermolabile and moderate thermostable elements of Klenow-like DNA Pol I in order to elucidate factors that induce thermal unfolding of both proteins by MD simulation.[18,19] We found similarity in the early stage of the unfolding process in both proteins. The unfolding was initiated by the breaking of electrostatic interactions at the interface between 3′→5′ exonuclease and 5′→3′ polymerase domains. In this study, we successfully distinguished thermostability level based on the number of electrostatic interactions at the domain interface. The number of interdomain electrostatic interactions in moderately thermostable DNA Pol I is higher than that of its thermolabile counterpart. Comparison of several thermophilic proteins indicate that there is a correlation between electrostatic interaction and the thermostability of proteins.[15,20,21] In order to confirm such a profile, in the present study we performed a similar simulation method using a more thermostable DNA Pol I *Taq,* ie, Klentaq1. We show here that interface domains of Klentaq1 are stabilized by higher numbers of electrostatic interactions compared to thermolabile elements, thereby strengthening the correlation between the number of electrostatic interactions at the interface domain and the thermostable property of DNA Pol I.

Materials and Methods

System preparation

Initial coordinates for the Klentaq1 structure were obtained from the Protein Data Bank website

(http://www.rscb.org)[22] with the entry code of 1QSS.[12] The deoxynucleoside triphosphate (dNTP) was removed from the complex enzyme using Visual Molecular Dynamics (VMD) software,[23] thereby leaving the apoenzyme. This apoenzyme was used as the initial structure of the enzyme throughout the simulations.

Molecular dynamics simulation parameters

All simulations were performed by the simulated annealing with nuclear magnetic resonance-derived energy restraints (SANDER) module of the Assisted Model Building with Energy Refinement (AMBER) 9.0 program.[24] Potential forces working on individual atoms were calculated using the AMBER force field (the Parm99 + frcmod ff03).[25] The implicit solvent (initial value for the generalized born; igb = 5) was used to describe the effect of solvent in MD simulation.[26] The mbondi2 radii and the reaction field cutoff (rbmax = 16) were employed to speed-up calculation of effective Born radii. In order to improve simulation efficiency, only those bond lengths involving hydrogen atoms were constrained with the SHAKE algorithm.[27] The protein consisted of 539 amino acid residues with a net molecular charge of about −8. The system was neutralized using 0.5 M NaCl. Temperature and pressure of the system were controlled using a Berendsen heat bath[28] and the external pressure of the bath was maintained at 1 atm, with relaxation time of 4 ps, respectively. The structure was first subjected to 5000 steps of energy minimization comprised of 500 steps by the steepest descent method, and then followed by the conjugate gradient to remove bad van der Waals contact. The trajectories and coordinates were saved every 1 ps with a 2 fs time step for structural analysis. MD trajectories of corresponding atoms were extracted using PTRAJ program. All images of the simulation systems and visualization of the structure were produced using VMD software.

Free energy calculation

The free energy perturbation (FEP) was calculated using the alchemical free energy method implemented in Scalable Molecular Dynamics (NAMD) 2.6.[29] The system was initially soaked in a cubic box ($50 \times 50 \times 50$ Å^3) of TIP3P water model.[30] A topological file containing hybrid amino acids for all point mutations was created with a VMD plugin called Mutator, based on standard Chemistry at HARvard Molecular Mechanics (CHARMM) topology.[31] The solvated system was equilibrated to the simulation temperature and 1 bar of pressure, and then run for FEP simulation in the isothermal-isobaric (NPT) ensemble. Electrostatic forces were calculated using Particle Mesh Ewald (PME) method.[32,33] Ten Langevin dynamics simulations were performed with $\delta\lambda$ of 0.1. The FEP calculations were run up to λ values of 1.0. In each λ, 50000 MD steps were carried out. The trajectories were saved every 2 fs.

Results

Conformational motion of Klentaq1

Thermostability of Klentaq1 was evaluated by performing the MD simulation at various temperatures using the implicit solvent model. Four different temperatures were set, including 300, 350, 373 and 400 K, to model temperature effects on the Klentaq1-structure. The simulation at 300 K was carried out to validate the setting parameters used in the entire simulation, and as reference for the native structure of the protein. The validated parameters at 300 K were then used for the other temperatures to simulate thermal unfolding of the protein.

The simulation result at 300 K was analyzed using a root-mean-square deviation (RMSD),[34] secondary structure composition, solvent accessible surface area (SASA) and B-factor in order to check the applied simulation parameters against the stability of Klentaq1. The RMSD analysis of the backbone atoms at 300 K showed that values converged at the relatively low level of 5 Å, indicating the protein conformation was less deviated from its initial structure (see Fig. 1). In terms of secondary structure composition, we found that α-helix and β-sheet contents were almost steady along the simulation time range. The same pattern was also found in the SASA profile; its value was almost constant at 300 K (data not shown). Both analyses suggest that the protein conformation was stable at secondary and tertiary structures. Further analysis was carried out to measure residual mobility of the protein by calculating root-mean-square fluctuation (RMSF) of Cα in each residue. RMSF of residues reflect flexibility/rigidity regions where those residues reside in the protein structure. The obtained RMSF value was the converted into B-factors and mapped onto the structure of protein.

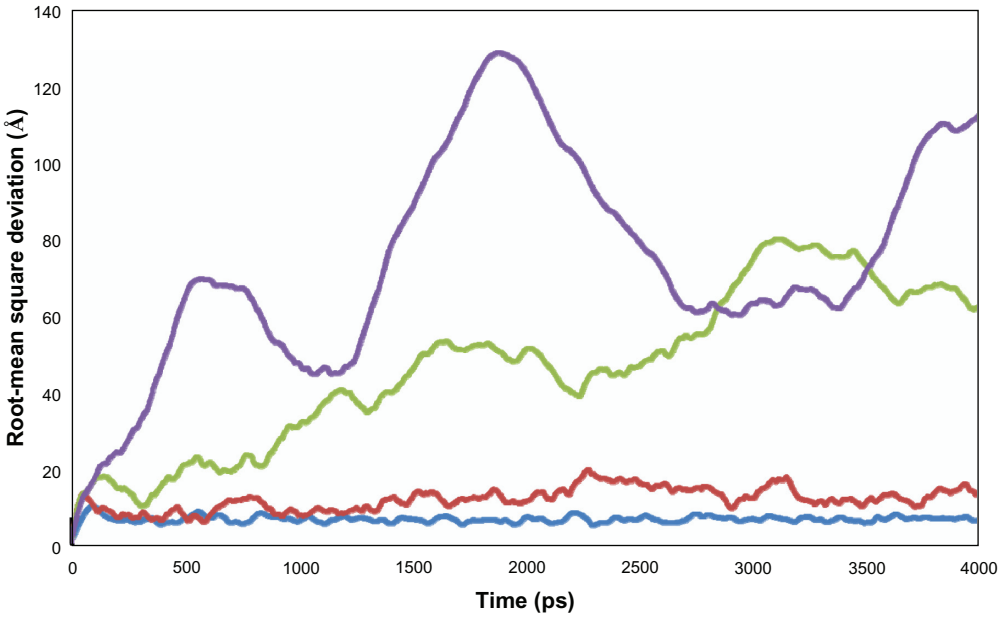

Figure 1. Root-mean-square deviation (RMSD) values of the Cα of Klentaq 1 at various temperatures as a function of simulation time.
Notes: Blue line, RMSD at 300 K; Red line, RMSD at 350 K; Green line, RMSD at 373 K; and Purple line, RMSD at 400 K.

The map (see Fig. 2) suggests that amino acid residues in Klentaq1 are stable during simulation at 300 K. All analyses above thus confirm the validity of simulation parameters used in our study; therefore they were used in whole simulations carried out in this study.

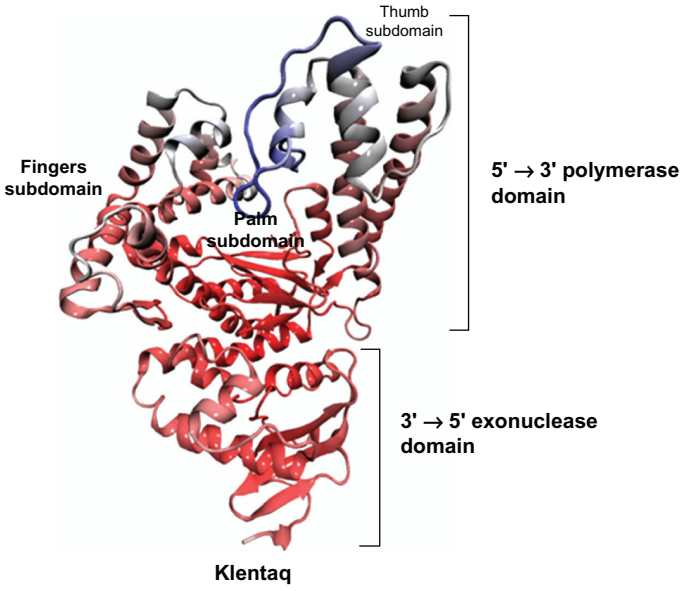

Figure 2. Thermostability map of Klentaq1 based on B-factor value for 300 K simulation.
Notes: The thermostability map was illustrated in RGB (Red Green Blue) color scale, where the rigid (stable) to flexible region is showed as a gradation in color from red to blue. The backbone atoms are displayed as a new ribbon to show the secondary structure (Drawn with VMD).

Early unfolding process of Klentaq1

Evaluations of thermal unfolding simulations of Klentaq1 were performed at 350, 373 and 400 K. Simulation at 350 K was chosen based on Barnes[4] to mimic the natural temperature for polymerization. Barnes[4] reported that the optimum temperature of Klentaq1 for polymerization was about 343–348 K, whereas the thermal denaturation (T_m value) based on differential scanning calorimetry (DSC) was 373 K.[35] The 400 K temperature was selected to observe the effect of higher temperatures on the unfolding process of Klentaq1.

The RMSD of Cα was measured at the above temperatures and the results are shown in Figure 1. The RMSD at 400 K showed a sharp increase up to 65 Å early in the simulation (~600 ps) suggesting that the structure of the protein was disrupted. In contrast, the RMSD profile at 350 K yielded values that were constant during 10 Å to 12 ns of simulation. Meanwhile, the profile at 373 K increased smoothly and reached up to 60 Å after 4 ns. Further analyses on conformational stability at 350 and 373 K were carried out by evaluation of the SASA and secondary structure composition. These results showed that the α-helix and β-sheet at 350 K were gradually decreased, for the α-helix from 50% to 45% and for the β-sheet 11% to 10%, while the profile of the total SASA values was increased from 30000 Å^2 to 40000 Å^2 after 3 ns

(data not shown). In contrast, the percentages of the secondary structure at 373 K sharply decreased from 50% to 30% for the α-helix and from 13% to 2% for the β-sheet after 4 ns of simulation (see Fig. 3A). To investigate detailed tertiary structure stability, each parameter of SASA values such as the whole surface area, polar region, non-polar region, and backbone of protein, was calculated. Each of these values was sharply increased after 1 ns simulation (see Fig. 3B). These results suggest that temperature at 373 K can

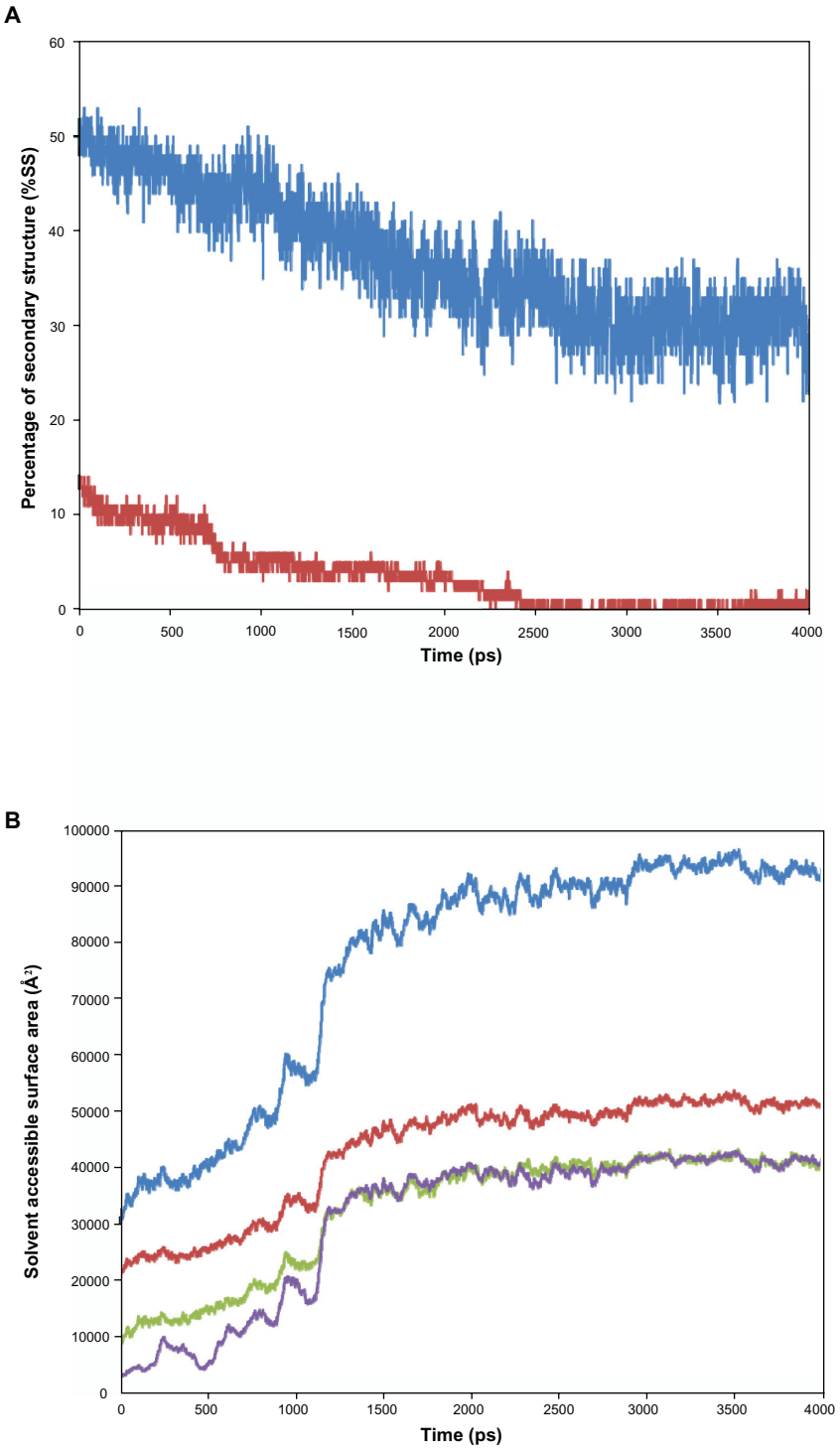

Figure 3. (**A**) Percentage of secondary structure for Klentaq1 during 373 K simulation, α-helix (blue line) and β-sheet (red line). (**B**) Solvent accessible surface area (SASA) values for the total area (blue line), polar region (red line), non-polar region (green line) and backbone (purple line) of Klentaq1 during 373 K simulation.

be further used to analyze detailed conformational instability of Klentaq1.

Several unfolding trajectory snapshots were also analyzed in order to examine qualitative conformation. Snapshots of Klentaq1 at 373 K indicate that the unfolding was a stepwise process (see Fig. 4). The 3D structure of protein is stable up to 250 ps. Local changes, especially at the thumb and fingers subdomains, appeared at 250 to 750 ps. Beyond 750 ps, the thumb subdomain was disrupted followed by domain separation after 1 ns of simulation (see Fig. 4). The unfolding snapshot was consistent with the RMSD and SASA values observed. These data suggest that the unfolding process of Klentaq1 is initiated by disruption of fingers and thumb subdomains, followed by separation between 3′→5′ exonuclease and 5′→3′ polymerase domains.

Domain integrity and thermostability

In order to elucidate factors responsible for maintenance of interdomain integrity, we further analyzed the simulation trajectory of the thermal unfolding simulation at 373 K, particularly at the event of domain separation between 3′→5′ exonuclease and 5′→3′ polymerase domains. The critical event in the interdomain separation was found when two buried salt bridges formed by pairs of Asp371-Arg435 (I) and Lys354-Glu445 (II) were disrupted (see Figs. 4 and 5). The electrostatic interaction distance of each pair was monitored and the results showed that the distance between these interactions was initially constant at around 2 Å up to 400 ps, then increased slowly up to 8 Å, and then sharply increased up to 100 Å until after 2 ns of simulation (see Fig. 5). These data were consistent with the snapshot result, suggesting that the domains are intact until 400 ps. They were found since the distance between the opposite charged residues in each salt bridge separated within a similar time range to the sharp increase in RMSD and SASA (see Figs. 1 and 3B).

In order to further identify the important role of electrostatic interactions at interface domains, in silico mutations were carried out to create a variety of mutants. Four hypothetic mutants were created to evaluate interactions (I) and (II), ie, Asp371Glu, Asp371Asn, Glu445Gln and Glu445Asp (see Table 1). The Gibbs free energy solvation ($\Delta\Delta G_{solv}$) of mutants was calculated using FEP methods and their values were compared with the wild type. The Asp371Glu (I.1), Asp371Asn (I.2), and Glu445Gln (II.2) mutants

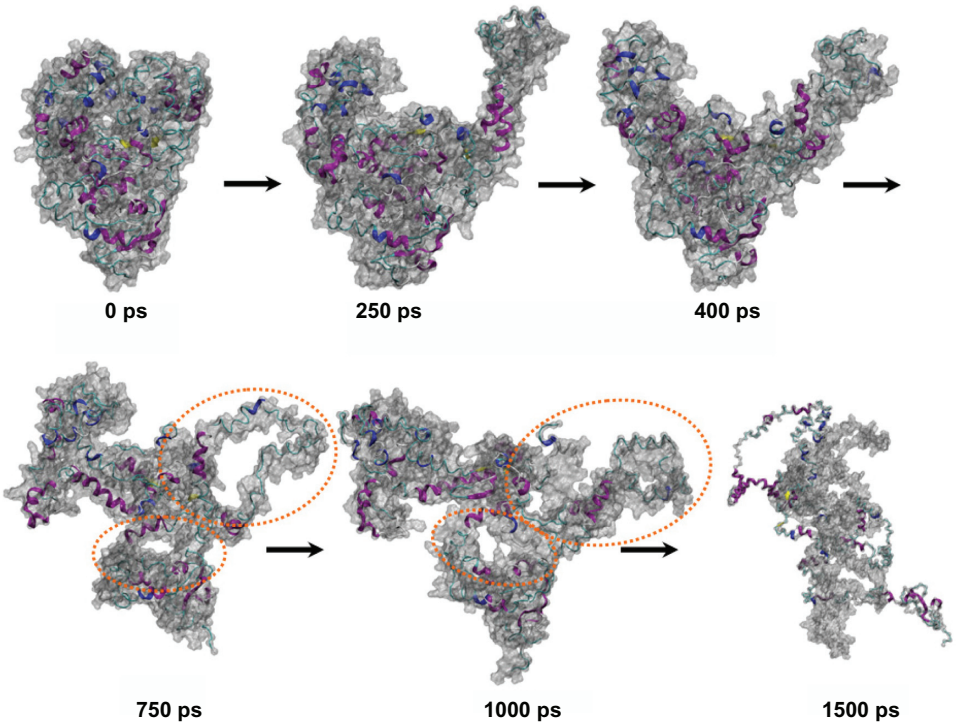

Figure 4. Conformational changes in Klentaq1 observed in the unfolding profile at 373 K simulation.
Note: The circles indicate early events in the unfolding process (Drawn with VMD).

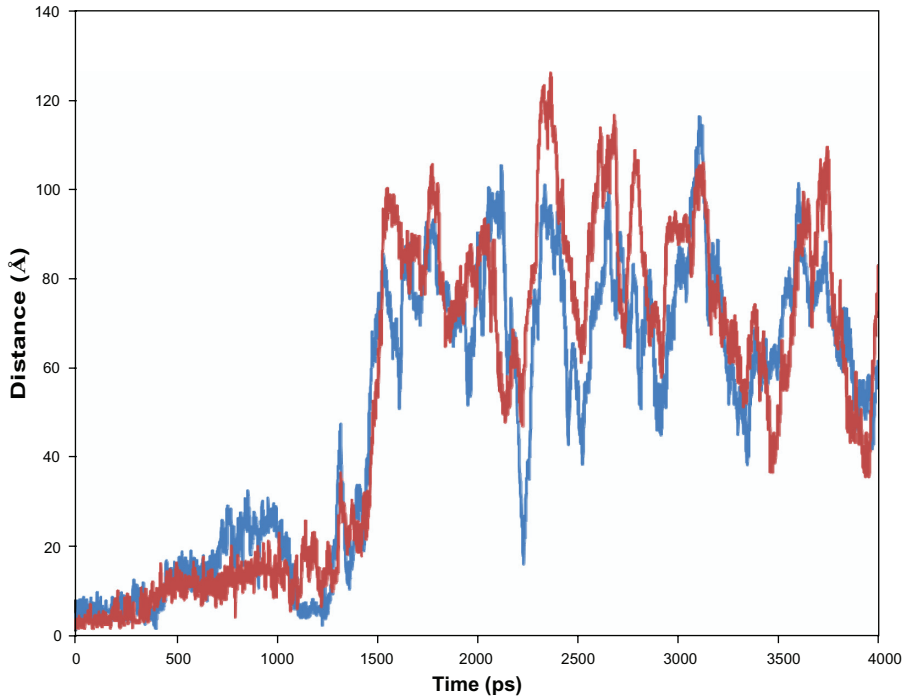

Figure 5. The distance of electrostatic interaction (salt bridges) ie, Asp371-Arg435 (blue line) and Lys354-Glu445 (red line) during 373 K simulation.

showed positive values of $\Delta\Delta G_{solv}$. These values were 25.94, 63.45, and 56.57 kcal/mole respectively (see Table 1), suggesting that these mutants were less stable compared to the wild type. In contrast, the Glu445-Asp (II.1) mutant showed a negative value of $\Delta\Delta G_{solv}$ (–20.72 kcal/mole), suggesting that this mutant was more stable than the wild type.

Discussion

Thermostability is the description of how a protein unfolds globally in response to thermal energy, but still retains its catalytic function.[17] Proteins and enzymes from thermophilic microorganisms offer good model systems by which to study the origins of thermostability.[36] Various factors have been shown to contribute to the thermostability of a protein from thermophiles, such as increased packing density, increased core hydrophobicity and decreased flexibility of the loop region.[37,38] These factors have been studied through both experimental (mutagenesis study) and computational methods.[39] The use of a computational approach provides deeper insight into atomic motion in protein structure and dynamic behavior of enzymes.[40–42] Based on computational methods, thermostability can be studied by performing high temperature simulation to denature the protein, namely thermal unfolding simulation.[43] In this report, MD simulations of Klentaq1 at elevated temperatures were performed to elucidate factors governing the stability of protein conformation.

Table 1. The Gibbs free energy solvation ($\Delta\Delta G_{sol}$) of mutants.

Pairs of interactions	$\Delta\Delta G_{solv}$ (kcal/mole)	Type of interaction	Name of mutant
Asp371-Arg435 (I)			
Mutant			
Glu371-Arg435 (I.1)	25.94	Electrostatic	Asp371Glu
Asn371-Arg435 (I.2)	63.45	Hydrogen bond	Asp371Asn
Lys354-Glu445 (II)			
Mutant			
Lys354-Asp445 (II.1)	–20.72	Electrostatic	Glu445Asp
Lys354-Gln445 (II.2)	56.57	Hydrogen bond	Glu445Gln

Throughout the simulations in this study, we used an implicit solvent system instead of an explicit one. The implicit model provides an adiabatic solvent response that is important for the fast unfolding simulation.[44] Therefore, we can probe factors responsible for interdomain integrity within a relatively short time. This is because when one uses an implicit solvent, the viscosity of a system is very low and almost null due to the lack of frictional force of water molecules. This means that the unfolding process of the protein will occur rapidly under elevated temperature.[45] It has been reported elsewhere that simulation in an implicit solvent has comparable accuracy to simulation conducted in an explicit solvent. MD simulation carried out by Huang and Stultz[46] showed that the paired-helical filament 6 (PHF6) peptide in Tau protein simulated using an implicit solvent could accurately reproduce the set of local energy minimums resulting from explicit solvent simulation. Moreover, all implicit solvent models used by Huang and Stultz[46] demonstrated that PHF6 forms extended β-structures in solution, which is consistent with the experimental result that PHF6 forms intracellular aggregates causing Alzheimer's disease.[47]

It is shown above that the two electrostatic interactions/salt-bridges (Asp371-Arg435 and Lys354-Glu445) buried in the interface domain region play an important role in maintaining the stability of the interdomain integrity (Table 1). Our finding is supported by Korolev and colleagues[14] who suggested that electrostatic interaction at the interface domain between 3′→5′ exonuclease and 5′→3′ polymerase domains is a key factor for the thermostability of an enzyme, based on their 3D structure analysis of Klentaq1. By using a variation of salt concentration, the importance of electrostatic interaction is also found in KF.[48,49] However, the authors of the above study[14] did not mention the amino acid residues interactions that play a role in maintaining the stability of the enzyme. Studies of multidomain proteins also show the importance of interdomain interactions to protein stability, such as glycosyl hydrolase[50] and β- and γ-crystallin eye lens protein.[51] Glycosyl hydrolase is a multidomain enzyme that is similar to DNA Pol, consisting of a catalytic domain, a second catalytic domain with similar or different activity (bifunctional enzyme), substrate-binding domains, a surface-layer domain and a linker domain whose function is unknown.[52] Kataeva and colleagues[50] showed that domain interactions affect the thermostability of glycosyl hydrolase from *Clostridium thermocellum*. Furthermore, Vieille and Zeikus[15] suggested that interdomain or intersubunit interactions are a major mechanism of stability for most hyperthermophilic proteins, such as for glutamate dehydrogenase (GluDH) from *P.furiosus, P.kodakaraensis,* and *T.litoralis*.[53,54]

Our previous results[18,19] in thermolabile DNA Pol I (KF) and moderately thermostable DNA Pol I (Klenow-like DNA Pol I ITB-1) also suggested that interdomain interaction contributes to the stability of enzymes. Moreover, we also found that there was similarity in the early unfolding processes of these enzymes. The process initiated by domain separation between 3′→5′ exonuclease and 5′→3′ polymerase domains. The results also suggested that the unfolding process of an enzyme from a thermophilic microorganism was much slower than that of its mesophilic counterpart. This phenomenon might be due to the increase in electrostatic interaction at the interface domain; ie, 1 in KF and 2 in both of Klenow-like DNA Pol I ITB-1 and Klentaq1. The above results are also supported by findings regarding hyperthermostable GluDH. Isolated from *P.furiosus,* this contains 7 electrostatic interactions buried at interdomain interfaces. In contrast, the GluDH from mesophilic *Clostridium symbiosum* consists of only one electrostatic interaction at the interface domain.[55] Our previous results also suggested that Klentaq1 was more stable than the Klenow-like DNA Pol I ITB-1 since the unfolding process of Klenow-like DNA Pol I ITB-1 was faster than Klentaq1. These findings are also supported by experimental polymerization data,[4,56,57] which shows that *Bacillus* DNA Pol I has a lower polymerization temperature (around 60° C–65° C) compared to that of Klentaq1. The results of the MD simulation also suggest that these 2 enzymes (Klenow-like DNA Pol I ITB-1 and Klentaq1) have 2 pairs of electrostatic interactions[18] at their interface domains (Table 1). The interface domain interaction difference between both enzymes only differs in the second interaction; specifically, Asp371-Arg435 on Klentaq1. The Asp-Arg interaction is reportedly[15] better adapted to high temperature compared to the Lys-Glu interaction. This

might due to the finding that, at elevated temperature, Arg exhibits more stable maintenance of electrostatic interactions and a net positive charge, since the pK_a of Arg side chains are more basic (12.1) than Lys (11.1) (pK_a values drop as the temperature increase). As with Arg, the side chains of Asp (pK_a 3.9) are more acidic than Glu (pK_a 4.2) hence Asp will be more stable during maintenance of a net negative charge than Glu. The above conditions suggest that an electrostatic interaction formed by Arg-Asp would be stronger than an electrostatic interaction formed by Lys-Glu.[15]

Author Contributions

Conceived and designed the experiments: SN, RH. Analysed the data: SN. Wrote the first draft of the manuscript: SN. Contributed to the writing of the manuscript: SN, RH, Akh. Agree with manuscript results and conclusions: RH, MAM, Akh. Jointly developed the structure and arguments for the paper: SN, RH, MAM, Akh. Made critical revisions and approved final version: SN, RH. All authors reviewed and approved of the final manuscript.

Funding

The present work has partially been supported by research grant from Institut Teknologi Bandung (ITB) No 174/K0107/PL/2007 to RH and Institut Teknologi Bandung scholarship (voucher) to SN.

Competing Interests

Author(s) disclose no potential conflicts of interest.

Disclosures and Ethics

As a requirement of publication author(s) have provided to the publisher signed confirmation of compliance with legal and ethical obligations including but not limited to the following: authorship and contributorship, conflicts of interest, privacy and confidentiality and (where applicable) protection of human and animal research subjects. The authors have read and confirmed their agreement with the ICMJE authorship and conflict of interest criteria. The authors have also confirmed that this article is unique and not under consideration or published in any other publication, and that they have permission from rights holders to reproduce any copyrighted material. Any disclosures are made in this section. The external blind peer reviewers report no conflicts of interest.

References

1. Ito J, Braithwaite DK. Compilation and alignment of DNA polymerase sequences. *Nucleic Acids Res*. 1991;19(15):4045–57.
2. Patel PH, Loeb LA. DNA polymerase active site is highly mutable: evolutionary consequences. *Proc Natl Acad Sci U S A*. 2000;97(10):5095–100.
3. Rothwell PJ, Waksman G. Structure and mechanism of DNA polymerases. *Adv Protein Chem*. 2005;71:401–40.
4. Barnes WM. PCR amplification of up to 35-kb DNA with high fidelity and high yield from lambda bacteriophage templates. *Proc Natl Acad Sci U S A*. 1994;91(6):2216–20.
5. Kornberg A, Baker TA. *DNA Replication*. 2nd ed. New Jersey: University Science Books; 2005.
6. Chien A, Edgar DB, Trela JM. Deoxyribonucleic acid polymerase from the extreme thermophile Thermus aquaticus. *J Bacteriol*. 1976;127(3): 1550–7.
7. Suzuki M, Yoshida S, Adman ET, Blank A, Loeb LA. Thermus aquaticus DNA polymerase I mutants with altered fidelity. Interacting mutations in the O-helix. *J Biol Chem*. 2000;275(42):32728–35.
8. Kaledin AS, Sliusarenko AG, Gorodetskii SI. Isolation and properties of DNA polymerase from the extreme thermophilic bacterium Thermus ruber. *Biokhimia*. 1982;47(11):1785–91.
9. Lawyer FC, Stoffel S, Saiki RK, Myambo K, Drummond R, Gelfand DH. Isolation, characterization, and expression in Escherichia coli of the DNA polymerase gene from Thermus aquaticus. *J Biol Chem*. 1989;264(11): 6427–37.
10. Kim Y, Eom SH, Wang J, Lee DS, Suh SW, Steitz TA. Crystal structure of Thermus aquaticus DNA polymerase. *Nature*. 1995;376(6541): 612–6.
11. Eom SH, Wang J, Steitz TA. Structure of Taq polymerase with DNA at the polymerase active site. *Nature*. 1996;382(6588):278–81.
12. Li Y, Korolev S, Waksman G. Crystal structures of open and closed forms of binary and ternary complexes of the large fragment of Thermus aquaticus DNA polymerase I: structural basis for nucleotide incorporation. *EMBO J*. 1998;17(24):7514–25.
13. Ollis DL, Brick P, Hamlin R, Xuong NG, Steitz TA. Structure of large fragment of Escherichia coli DNA polymerase I complexed with dTMP. *Nature*. 1985;313(6005):762–6.
14. Korolev S, Nayal M, Barnes WM, di Cera E, Wakman G. Crystal structure of the large fragment of Thermus aquaticus DNA polymerase I at 2.5-Å resolution: structural basis for thermostability. *Proc Natl Acad Sci U S A*. 1995;92(20):9264–8.
15. Vieille C, Zeikus GJ. Hyperthermophilic enzymes: sources, uses, and molecular mechanisms for thermostability. *Microbiol Mol Biol Rev*. 2001; 65(1):1–43.
16. Bosshard HR, Marti DN, Jelesarov I. Protein stabilization by salt bridges: concepts, experimental approaches and clarification of some misunderstandings. *J Mol Recognit*. 2004;17(1):1–16.
17. Zhang JH, Zhang LL, Zhou LX. Thermostability of protein studied by molecular dynamics simulation. *J Biomol Struct Dyn*. 2004;21(5): 657–62.
18. Nurbaiti SN, Hertadi RH, Martoprawiro MA, Akhmaloka. The role of interface domain interactions on thermal stability of DNA polymerase I ITB-1. *The Open Structural Biology Journal*. 2009;3:16–25.
19. Nurbaiti SN, Hertadi RH, Martoprawiro MA, Akhmaloka. Interface domain interactions on early stage unfolding of DNA polymerase I Klenow fragment. *Int J Integr Biol*. 2009;6(1):46–51.
20. Yip KS, Stillman TJ, Britton KL, et al. The structure of Pyrococcus furiosus glutamate dehydrogenase reveals a key role for ion-pair networks in maintaining enzyme stability at extreme temperatures. *Structure*. 1995; 3(11):1147–58.

21. Karshikoff A, Ladenstein R. Ion pairs and the thermotolerance of proteins from hyperthermophiles: a "traffic rule" for hot roads. *Trends Biochem Sci*. 2001;26(9):550–6.
22. Berman HM, Westbrook J, Feng Z, et al. The protein data bank. *Nucleic Acids Res*. 2000;28(1):235–42.
23. Humphrey W, Dalke A, Schulten K. VMD: visual molecular dynamics. *J Mol Graph*. 1996;14(1):33–8, 27–8.
24. Case DA, Cheatham TE 3rd, Darden T, et al. The Amber biomolecular simulation programs. *J Comput Chem*. 2005;26(16):1668–88.
25. Duan Y, Wu C, Chowudhury S, et al. A point-charge force field for molecular mechanics simulations of proteins based on condensed-phase quantum mechanical calculations. *J Comput Chem*. 2003;24(16):1999–2012.
26. Onufriev A, Bashford D, Case DA. Exploring protein native states and large-scale conformational changes with a modified generalized born model. *Proteins*. 2004;55(2):383–94.
27. Ryckaert JP, Ciccotti G, Berendsen HJC. Numerical integration of the cartesian equations of motion of a system with constraints: molecular dynamics of n-alkanes. *J Comput Phys*. 1977;23(3):327–41.
28. Berendsen HJC, Postma JPM, van Gunsteren WF, Dinola A, Haak JR. Molecular dynamics with coupling to an external bath. *J Chem Phys*. 1984; 81(8):3684–90.
29. Phillips JC, Braun R, Wang W, et al. Scalable molecular dynamics with NAMD. *J Comput Chem*. 2005;26(16):1781–802.
30. Jorgensen WL, Chandrasekhar J, Madura JD, Impey RW, Klein ML. Comparison of simple potential functions for simulating liquid water. *J Chem Phys*. 1983;79(2):926–35.
31. Brooks BR, Bruccoleri RE, Olafson BD, States DJ, Swaminathan S, Karplus M. CHARMM: A program for macromolecular energy, minimization, and dynamics calculations. *J Comput Chem*. 1983;4(2):187–217.
32. Darden T, York D, Pedersen L. Particle mesh Ewald: An N. log(N) method for Ewald sums in large systems. *J Chem Phys*. 1993;98(12):10089–92.
33. Essmann U, Perera L, Berkowitz ML, Darden T, Lee H, Pedersen LG. A smooth particle mesh Ewald method. *J Chem Phys*. 1995;103(19):8577–93.
34. Becker OM, MacKerrel AD, Roux B, Watanabe M. *Computational Biochemistry and Biophysics*. New York: Marcel Dekker Inc; 2001.
35. Karantzeni I, Ruiz C, Liu C, Licata VJ. Comparative thermal denaturation of Thermus aquaticus and Escherichia coli type 1 DNA polymerases. *Biochem J*. 2003;374(Pt 3):785–92.
36. Strop P, Mayo SL. Contribution of surface salt bridges to protein stability. *Biochemistry*. 2000;39(6):1251–5.
37. Russell RJ, Ferguson JM, Hough DW, Danson MJ, Taylor GL. The crystal structure of citrate synthase from the hyperthermophilic archaeon Pyrococcus furiosus at 1.9 Å resolution. *Biochemistry*. 1997;36(33): 9983–94.
38. Jaenicke R, Böhm G. The stability of proteins in extreme environments. *Curr Opin Struct Biol*. 1998;8(6):738–48.
39. Sakasegawa S, Takehara H, Yoshioka I, et al. Increasing the thermostability of Flavobacterium meningosepticum glycerol kinase by changing Ser329 to Asp in the subunit interface region. *Protein Eng*. 2001;14(9): 663–7.
40. Lee MR, Duan Y, Kollman PA. Use of MM-PB/SA in estimating the free energies of proteins: application to native, inter-mediates, and unfolded villin headpiece. *Proteins*. 2000;39(4):309–16.
41. Arcangeli C, Bizzarri AR, Cannistraro S. Molecular dynamics simulation and essential dynamics study of mutated plastocyanin: structural, dynamical and functional effects of a disulfide bridge insertion at the protein surface. *Biophys Chem*. 2001;92(3):183–99.
42. Tejo BA, Salleh AB, Pleiss J. Structure and dynamics of Candida rugosa lipase: the role of organic solvent. *J Mol Model*. 2004;10(5–6):358–66.
43. Day R, Bennion BJ, Ham S, Daggett V. Increasing temperature accelerates protein unfolding without changing the pathway of unfolding. *J Mol Biol*. 2002;322(1):189–203.
44. Paci E, Karplus M. Unfolding proteins by external forces and temperature: The importance of topology and energetics. *Proc Natl Acad Sci U S A*. 2000;97(12):6521–6.
45. Ferrara P, Apostolakis J, Caflisch A. Thermodynamics and kinetics of folding of two model peptides investigated by molecular dynamics simulations. *J Phys Chem B*. 2000;104(20);5000–10.
46. Huang A, Stultz CM. Conformational sampling with implicit solvent models: application to the PHF6 peptide in tau protein. *Biophys J*. 2007; 92(1):34–45.
47. von Bergen M, Friedhoff P, Biernat J, Heberle J, Mandelkow EM, Mandelkow E. Assembly of tau protein into Alzheimer paired helical filaments depends on a local sequence motif ((306)VQIVYK(311)) forming beta structure. *Proc Natl Acad Sci U S A*. 2000;97(10):5129–34.
48. Astatke M, Ng K, Grindley ND, Joyce CM. A single side chain prevents Escherichia coli DNA Polymerase I (Klenow Fragment) from incorporating ribonucleotides. *Proc Natl Acad Sci U S A*. 1998;95(7):3402–7.
49. Richard AJ, Liu CC, Klinger AL, Todd MJ, Mezzasalma TM, LiCata VJ. Thermal stability landscape for Klenow DNA polymerase as a function of pH and salt concentration. *Biochim Biophys Acta*. 2006;1764(10): 1546–52.
50. Kataeva IA, Blum DL, Li XL, Ljungdahl LG. Do domain interactions of glycosyl hydrolases from Clostridium thermocellum contribute to protein thermostability? *Protein Eng*. 2001;14(3):167–72.
51. Flaugh SL, Kosinski-Collins MS, King J. Interdomain side-chain interactions in human gammaD crystallin influencing folding and stability. *Protein Sci*. 2005;14(8):2030–43.
52. Bayer EA, Shimon LJ, Shoham Y, Lamed R. Cellulosomes-structure and ultrastructure. *J Struc Biol*. 1998;124(2–3):221–34.
53. Rahman RN, Fujiwara S, Nakamura H, Takagi M, Imanaka T. Ion pairs involved in maintaining a thermostable structure of glutamate dehydrogenase from a hyperthermophilic archaeon. *Biochem Biophys Res Commun*. 1998;248(3):920–6.
54. Vetriani C, Maeder DL, Tolliday N, et al. Protein thermostability above 100 degreesC: a key role for ionic interactions. *Proc Natl Acad Sci U S A*. 1998;95(21):12300–5.
55. Yip KS, Britton KL, Stillman TJ, et al. Insights into the molecular basis of thermal stability from the analysis of ion-pair networks in the glutamate dehydrogenase family. *Eur J Biochem*. 1998;255(2):336–46.
56. Kiefer JR, Mao C, Hansen CJ, et al. Crystal structure of a thermostable Bacillus DNA polymerase I large fragment at 2.1 A resolution. *Structure*. 1997;5(1):95–108.
57. Akhmaloka, Pramono H, Ambarsari L, Susanti E, Nurbaiti S, Madayanti F. Cloning, homological analysis, and expression of DNA Pol I from Geobacillus thermoleovorans. *Int J Integr Biol*. 2007;1(3):206–15.